

Interaction of alkali metals with Si(001)-2×1

Inder P. Batra

IBM Research Division, Almaden Research Center (K62/282), 650 Harry Road, San Jose, California 95120-6099

(Received 24 January 1990)

An extensive set of total-energy and force calculations has been performed for alkali metals such as Na and K on Si(001)-2×1 at different coverages. Full lattice relaxation has been carried out in the presence of adsorbed overlayers at competing sites to arrive at a definitive structure. These results are compared with other theoretical and experimental results. A complete discussion of the 2×3 low-energy electron-diffraction structure and atop site assignment by scanning tunneling microscopy at low coverages is given. The compatibility of the structures with the negative-electron-affinity activation of Si(001)-2×1 is also pursued. We address issues such as interface metallicity, charge transfer, and bonding, using the results of our electronic-structure calculations. The metallic behavior at $\frac{1}{2}$ a monolayer coverage of alkali metals is emphasized by showing the Fermi line in the two-dimensional surface Brillouin zone. We also examine in depth the issue raised by a recent cluster-model calculation where the widely used quasihexagonal adsorption site is found to be unstable towards a zigzag Peierls type of Δx distortion of the alkali-metal overlayer. We studied in detail the energetics associated with this distortion for Na-Si(001)-2×1 at $\frac{1}{2}$ a monolayer coverage but found no instability of the quasihexagonal adsorption site. The apparent lack of agreement is explained in terms of incomplete nesting of the Fermi surface and alkali-metal-Si bonding. These findings are further confirmed upon deliberately altering the bonding by replacing Na with Al. At a monolayer coverage the two competing structural models, the so-called (*H-B*) and (*H-C*), cannot be distinguished on the basis of total energy in the presence of complete lattice relaxation. There is a tendency to lift the surface 2×1 reconstruction by stretching the dimer bond, but a complete reversal to ideal surface structure is found to be energetically unfavorable. This is to be contrasted with Al, which lifts the reconstruction at about $\frac{1}{2}$ a monolayer coverage. Our calculated electronic structure is compared with the angular-resolved photoemission data with K-saturated single-domain Si(001)-2×1. The observed reentrant behavior to an insulating state at the monolayer coverage of alkali metals can be explained equally well by both the models.

I. INTRODUCTION

It is well known that the deposition of alkali metals (AM's) at submonolayer coverages on semiconductors leads to a significant reduction of the work function. In particular, if the work function is lowered to such an extent that the vacuum level falls below the bulk conduction band, then the system is said to be driven in the negative-electron-affinity (NEA) state.¹ It was first reported¹ back in 1970 and confirmed² subsequently that the Si(001) surface can be activated to NEA by adsorption of AM (and subsequent addition of oxygen). These systems have important technological applications² as high-efficiency emitters and have since been actively pursued. Furthermore, AM-assisted oxidation of semiconductors has potential applications³ in the microelectronics industry. More recently, a school of thought emerged that since AM's when adsorbed on semiconductors do not react or interdiffuse with the substrate, they may serve to elucidate fundamental aspects of metallization⁴ so vital to the Schottky-barrier problem. Thus there is a flurry of activity both experimentally⁵⁻¹⁷ and theoretically.¹⁸⁻²⁵ Significant results have emerged along with some controversial findings which have made the study of interaction of AM's with semiconductors an area

of active research.^{4,26} In this manuscript we pursue the interaction of AM's like K and Na with the Si(001)-2×1 surface.

One of the early indications that the bonding of AM's to semiconductors may be different from their bonding to other metals came from the work-function (Φ) measurements.^{5,9,10,17} In general, for AM adsorption on other metals,²⁷⁻³⁰ Φ decreases almost linearly at low coverages, passes through a minimum, and then rises to a saturation value which corresponds to Φ of the bulk AM. For AM on the semiconductors there are reports^{5,17} of the absence of the minimum in work function. In any case, when a minimum is observed, it occurs^{9,10,31,32} at coverages higher than those typically reported for the AM-metal systems.

Another difference from metals is the observation that at room temperature, AM's on Si(001)-2×1 lead to a saturated overlayer. The value of the saturation coverage itself, however, is unsettled. Based on a strong 2×1 low-energy-electron-diffraction (LEED) pattern at saturation, several authors^{5,17,33,34} have inferred the saturation coverage for K on Si(001)-2×1 at room temperature to be $\frac{1}{2}$ of a monolayer (ML). Enta *et al.*,⁹ on the other hand, from their angular-resolved ultraviolet photoemission spectroscopy (ARUPS) data have concluded that the sat-

uration coverage is 1 ML. Abukawa and Kono¹⁰ have also concluded, based on a kinematical analysis of the x-ray photoelectron diffraction patterns of K $2p$ core levels, that the saturation coverage is 1 ML. Oellig and Miranda⁷ assert that the coverage can be much higher at room temperature. In fact, based on the interpretation that their Si *LMM* Auger-electron spectroscopy (AES) intensity data show at least four breaks, they claim a layer-by-layer growth of K on Si(001). This claim has been challenged by Enta *et al.*⁹ based on their own $\Delta\Phi$ and AES data.

The maximum reported coverage is problematic due perhaps to strong temperature dependence^{16,17} of the coverage around room temperature. Since a monolayer coverage has been defined differently in the literature, to avoid any confusion, we let Θ be the number of alkali-metal atoms per Si(001)-2×1 surface unit cell. Therefore 1 ML (or $\Theta=2$) coverage corresponds to 6.78×10^{14} adsorbates/cm² in our definition. It has been reported¹⁶ that around 300 K, a slight variation in the actual temperature of the sample can result in a different AM coverage. For example, at 273 K, 1 ML may be stabilized while at 325 K the saturation coverage is in between 0.5 and 1 ML.

The situation has been clarified by the more recent detailed LEED, $\Delta\Phi$, and AES measurements for Na/Si(001) by Glander and Webb.¹³ They performed two types of experiments which they called “dosing” and “equilibrium” experiments. In the former type, which are the more usual kind of experiments, the observations are made as a function of time after turning on a constant atomic beam flux on a substrate held at a fixed temperature. These types of experiments may also be characterized as transient as opposed to “equilibrium” or steady state where coverage is changed by varying the crystal temperature for a fixed AM flux; the temperature of the sample is changed slowly enough to ensure that adsorbates are in a steady state (desorption and adsorption rates are equal). They conclude that for wide range of effective pressures and temperatures the sticking coefficient changes abruptly from 1 to 0 at the saturation coverage of 0.68 ML of Na. One can grow bulk Na in islands only at low temperatures and high pressures.

The LEED data on AM/Si(001) appear to have consensus at least as far as the dominant features are concerned. The clean 2×1 structure changes^{13,33} to a third-order structure (2×3 or 3×2) and finally back to 2×1 structure at saturation coverage with spot intensities different from that for the clean surface. There are reports of 4×1 structure at 0.25 ML in dosing experiments¹³ and occasionally 2×3 LEED patterns have not been observed.¹⁶ Glander and Webb¹³ have also noted an incommensurate phase between 2×3 and 2×1 as a function of increasing coverage.

The nature of AM-semiconductor bond as a function of coverage is not fully understood yet. For AM on metals, Langmuir,³⁵ Gurney,³⁶ and more recently Lang²⁸ presented a model involving an ionic to metallic transition as a function of AM coverage. At low coverages, the AM atoms are largely ionized with the alkali valence s level (broadened into a resonance) appearing above E_F .

With increasing coverage, the depolarization effects shift the resonance downwards leading to a partial occupancy of the adatom s level. At sufficiently high coverage the AM overlayer turns metallic with a partially filled^{29,37} s band. Some recent calculations³⁰ have firmly established that the AM-metal bond has some covalent component even at low coverages and it should be more precisely viewed as a polarized bond as opposed to a strictly ionic bond.

For AM semiconductors the situation is even more complex.^{4,18,26} Some of the publications suggested^{6–8} that the AM-metal picture can be literally taken over for AM-semiconductor interactions as well. This view is not universally accepted. It is argued^{18,22,26} that the presence of active dangling bonds on semiconductor surfaces either delays (to higher coverages compared to overlayer on metals) or suppresses the overlayer metallization altogether. Published^{18–25} values of charge transfer (ΔQ) from AM to Si have varied from $0 < \Delta Q < 1$. Thus the AM-semiconductor bond has been alternatively characterized as strong ionic^{18,24} or weak covalent.¹² One also needs to know whether the interface is metallic or semiconducting. At a deeper level, one must resolve if the metallicity (when observed) is due to partially filled AM bands or due to partial occupancy of the substrate dangling bonds.

The optimum adsorption site for AM on Si(001)-2×1 at various coverages is still being actively investigated.^{23–25} Levine³³ in 1973 proposed for Cs adsorption on Si(001) that at low coverages this metal occupied a quasihexagonal hollow site (H) above the rows of dimers as shown in Fig. 1(a). The H site offered a simple explanation for the NEA (Refs. 33 and 38) because oxygen atoms could submerge under the long bridge (B) sites to cause additional (beyond that produced by AM) lowering of the work function required to achieve NEA. Since then this adsorption site has been widely used for other adsorbates as well, in qualitative discussions of various properties of AM/Si(001) interfaces. Most of the LEED data are consistent^{13,33,34} with this adsorption site as are the inverse photoemission data.¹¹

Scanning tunneling microscopy (STM) experiments have been performed recently^{39–41} on various AM-semiconductor systems. These include Cs-GaAs(110) and K,Li on Si(001)-2×1. The STM data on Cs-GaAs(110) were interpreted³⁹ in terms of a periodic one-dimensional Cs chainlike structure. Hashizume *et al.*⁴⁰ from their STM data have suggested that at low coverages, Li, K atoms are adsorbed in on the top (T) site above one of the dimer-forming Si atoms. But at about 0.1 ML coverage AM's formed linear chains perpendicular to the Si dimer rows. STM work by Badt *et al.*⁴¹ on K-Si(001)-2×1 noted considerable disorder. Also absent were any long chains of K atoms.

Another experiment^{15,16} directly dealing with the adsorption site of K on Si(001) is through titration physisorbed Xe. From this it was concluded that the long bridge site B [see Fig. 1(a)] is preferentially filled over an H site at $\frac{1}{2}$ ML coverage. This experiment requires a precise knowledge of the Xe thermal desorption spectra and correlation of various peaks with the surface adsorption

sites. Unfortunately, this is not known in an unambiguous^{15,16} fashion. In addition to the site there is also a lack of agreement on the value of the K—Si bond length. Values in the range of 2.6–3.5 Å have been published.^{18–25} There is only one direct measurement¹² for the K—Si bond length which gave a value of 3.14 ± 0.10 Å. This has been derived from surface-extended x-ray-absorption fine structure (SEXAFS) data¹² but is not site specific.

The conclusions drawn from various calculations^{18–26} are also somewhat diverse. Early theoretical work¹⁹ did not carry out total energy calculations. They accepted the *H* site as a given but varied the vertical height of the AM overlayer to obtain agreement with some measured property. The K—Si bond length, $d = 3.52$ Å, was inferred. Subsequently, results were presented²⁰ for several values of d .

The first total energy calculation for the *H* site was performed by Ciraci and Batra¹⁸ using the pseudopotential

method. They deduced an optimized value of $d = 2.6$ Å. The Si-K interatomic distance might be underestimated in these calculations due to the particular form of the ionic pseudopotential and possibly due also to the form of the exchange-correlation potential. The emphasis of the calculation was on metallization aspects rather than on precise structural evaluation. A calculation²¹ based on the pseudofunction method obtained a d of 3.32 Å at the *H* site. A small cluster-model calculation²² based on the self-consistent-field (SCF)–Hartree-Fock method again performed for the *H* site showed that the minimum in total energy as a function of vertical height of K was rather shallow. This was offered as an explanation for a range of published d values. The authors²² stated an optimum $d = 3.52$ Å. Although this value of d is even larger than the sum of covalent radii (3.3 Å) the bond was shown to be highly ionic. The authors²² therefore cautioned against deducing¹² the nature of the bond from the value of the bond length.

The relative stability of various sites was first examined by Batra²³ for Na-Si(001)- 2×1 . The basic conclusion was that the *H* and *B* sites are equally favored as far as the adsorption energy is concerned. Ling *et al.*²⁴ have recently carried out extensive cluster-model calculations for the K-Si system within the framework of local-density total energy formalism. In agreement with our earlier theoretical results,¹⁸ they found strong ionic bonding at both the competing *H* and *B* sites. For example, at the *H* site they obtained $\Delta Q \sim 0.63e$ from K to Si and a binding energy of about 3 eV. Their computed value of $d(\text{K—Si}) \sim 3.2$ Å is also close to the sum of atomic radii but again the bond has large ionicity. They noted that the adsorption at the *H* site is actually unstable to a zigzag distortion of K atoms and concluded that the *B* site is more stable than the *H* site. It should be noted that a reliable conclusion at the *B* site demands extreme numerical accuracy in the calculation. For example, the calculated change in energy was²⁴ only 0.002 eV when the vertical height of the K was changed by 0.1 a.u. around the equilibrium position. They also examined other sites and obtained total energies (in the order of decreasing stability) $E(B) < E(C) < E(H) \approx E(D)$. The corresponding $d(\text{Si—K})$ calculated by them in the same order are 3.2, 3.5, 3.2, and 3.1 Å.

More recently, a slab calculation²⁵ based on SCF–Hartree-Fock–incomplete neglect of differential overlap (INDO) scheme has also examined the relative stability of the four sites and obtained the same filling order: *B*, *C*, *H*, and *D* at $\frac{1}{2}$ ML coverage. The calculated $d(\text{Si—K})$ values, however, are 2.65, 3.34, 2.69, and 2.52 Å, respectively. Another key variance from the cluster-model results²⁴ is in the spread of total energy, i.e., the difference in total energy between the most and the least stable site. Whereas Ling *et al.*²⁴ report a spread of about 0.75 eV, the value by Ramirez²⁵ is about 5 eV.

At saturation coverages, Abukawa and Kono¹⁰ have proposed the existence of a K double layer. These results were based on a kinematical analysis of the x-ray photoelectron diffraction patterns of K *2p* core levels. They found that placing K atoms in (*H*-*C*) sites simultaneously (see Fig. 1) in a puckered configuration successfully ex-

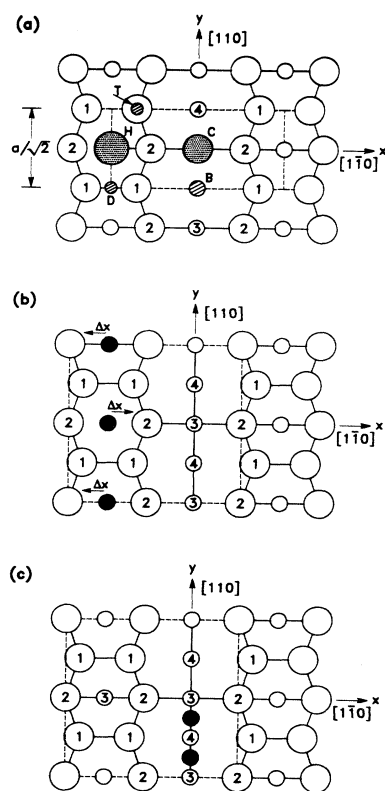


FIG. 1. Top views describing the positions of alkali metals (AM's) on Si(001)- (2×1) . Solid and empty circles denote AM and Si atoms, respectively. Numerals in the circles indicate Si atomic layers. (a) *H*, *B*, and *C* sites have been labeled in the 2×1 unit cell shown by dashed lines. At $\frac{1}{2}$ ML coverage ($\Theta = 1$) only one of these sites is occupied. At 1 ML ($\Theta = 2$) *H*-*B* or *H*-*C* are simultaneously occupied. (b) The 2×2 unit cell shown by dashed lines used to study the Δx Peierls distorted structure of AM at $\Theta = 1$. (c) The 2×2 unit cell shown by dashed lines used to study pairing of AM atoms (Δy distortion) of AM at $\Theta = 1$.

plained their observations. The dilayer corresponds to a coverage of 1 ML. This model has been supported by the calculations of Tsukada *et al.*²⁰ Batra,²³ based on pseudopotential calculations, has proposed the (*H-B*) model. Ramirez²⁵ has also found that the (*H-B*) model is 1.1 eV/(unit cell) more stable than the (*H-C*) model.

Incidentally, none of the calculations reported to date has allowed for the substrate relaxation,⁴² a defect we shall remedy in the present paper. The rigid substrate model would be a reasonable approximation if it were not for the fact that the atomic geometry of the Si(001)-2×1 surface is still not completely known.⁴³⁻⁴⁵ There is a lack of agreement⁴³⁻⁴⁵ as to whether the Si dimers are symmetric and/or buckled. One does not necessarily expect a significant lattice rearrangement due to the presence of AM. But since the substrate geometry itself is uncertain, the optimization of the entire system becomes essential. We show that the optimization leads to conclusions which are significant for site selectivity.

Many of the issues outlined above can be resolved or at least can be put in perspective from our total energy, atomic forces, and electronic-structure calculations. We have performed a number of calculations for Na,K adsorption on Si(001) at two coverages, $\Theta=1$ and 2, on various surface sites. For initial atomic positions for atoms in the substrate we used Si(001)-2×1 geometry as given by Abraham and Batra⁴⁴ (AB) and more recently by Batra.⁴⁵ We then optimized geometries in the presence of AM overlayers placed at various adsorption sites. We have also performed several calculations with a 2×2 unit cell to examine the Peierls type of distortion suggested by Ling *et al.*²⁴ for the quasihexagonal site. We also present a fully optimized model at the quasihexagonal adsorption site and show how much the substrate relaxes due to the presence of the AM overlayer. We also carry out the lattice relaxation for (*H-B*) and (*H-C*) models at $\Theta=2$. We compare our calculated electronic structure with the recent ARUPS data on a single domain Si(001)-2×1 and show that the two models cannot be distinguished on the basis of the comparison.

II. MODELS AND CALCULATIONS

We have investigated all the structural models shown in Fig. 1. We have chosen x [1 $\bar{1}0$] along the dimerization direction and z as normal to the surface along the [001] direction. Planes of Si atoms are labeled by numerals 1-4. Atoms labeled 1 normally have two dangling bonds each for an ideal bulk truncated structure. The 2×1 structure results when these atoms dimerize along the x direction forming rows of dimers along the y [110] direction.

We considered the five different registry patterns for the AM overlayer at the 2×1 surface at $\theta=1$. These arise from the placement of alkali metals above different symmetry sites on the Si(001)-2×1 surface. The hollow site, *H*(4,2,1), above the third layer of Si is quasihexagonal. The numbers in parentheses give the number of Si neighbors in the first three Si layers around the adsorption site. In the long bridge site, *B*(2,4,2), the adsorbate is located above a fourth layer Si atom and connects the

Si dimer rows. In the dimer bridge site, *D*(2,4,2), the adsorbate is above the midpoint of the Si dimer and in the top site, *T*(1,2,4), the adsorbate is above one of the dimer-forming atoms. The cave site, *C*(4,2,2), has adsorbate above the third layer of Si and due to reconstruction this is a more open site than *H*(4,2,1). Also, as can be seen in Fig. 1, the second layer Si atoms are in fact closer to the adsorbate than the first layer Si atoms. This is indicated by placing a hat above 2. These sites are simply labeled as *H*, *B*, *C*, *D*, and *T* in Fig. 1(a).

We must also consider the adsorption on the ideal surface to ensure that the 2×1 reconstruction is not lifted upon AM adsorption. On ideal surface, *B* and *D* sites are equivalent as are *H* and *C*. One can still get a 2×1 pattern at the ideal surface if adsorbates skip adjacent equivalent sites. Thus on an ideal surface we investigate the AM induced 2×1 reconstruction. The AM's were placed at *H*(*C*), *B*(*D*), and *T* sites.

Recently, Ling *et al.*²⁴ have proposed, based on cluster-model calculations, that an adsorbate in an *H* site is unstable towards a Peierls type of distortion. According to them, if alkali metals are moved away from the *H* sites by equal and opposite amounts (Δx) along the x direction [see Fig. 1(b)] the resultant structure is lower in energy. To investigate this structural model we considered a 2×2 periodic cell shown in Fig. 1(b) which has twice the area of the conventional 2×1 surface cell. This represents a fairly major computational effort since it contains 42 atoms per unit cell coupled with the fact that a large number of structures were to be explored. Incidentally, calculations on the 2×2 cells enable us to check the sensitivity of our results to the input calculational parameters.

We also studied the structure shown in Fig. 1(c), which considers the possibility of AM pairing at the *B* sites along the y direction (Δy distortion). This distortion places metal atoms in rows at right angles to Si dimer rows. Such pairing of metal atoms has been found to be energetically beneficial⁴⁶ for metals like Al and Ga on Si(001) and is in accord with experimental observations.^{47,48}

The structural models discussed above correspond to $\Theta=1$. At the higher coverage ($\Theta=2$) there are only a few plausible structures which can give the observed 2×1 LEED patterns. One involves simultaneous occupancy of *H* and *B* sites, the (*H-B*) model. An alternative involves occupying *H* and *C* sites simultaneously, the (*H-C*) model. This structure has been independently proposed^{9,10,26} by two different groups. Simultaneous occupation of *B* and *C* sites can be ruled out on physical grounds. We must also establish that reverting to the ideal surface is energetically unfavorable even at $\Theta=2$. This requires placing AM at *H-B* sites on the ideal unreconstructed surface since this can also give rise to a 2×1 LEED pattern. This structural model shall be denoted by *I*(*H-B*). There is no need to consider *I*(*H-C*) because on the ideal surface *H* and *C* sites are equivalent and this would correspond to a 1×1 structure.

All calculations of the total energies and Hellmann-Feynman forces were performed using a standard SCF-pseudopotential method^{49,50} within the framework of the

local-density functional theory applied in momentum space.⁴⁹ We employed the nonlocal, norm-conserving ionic pseudopotentials given by Bachelet *et al.*,⁵¹ using the Ceperly-Alder exchange and correlation potential⁵² as parametrized by Perdew and Zunger.⁵³ More details about the calculations can be found elsewhere.⁵⁴ The silicon substrate was simulated by a slab consisting of eight atomic layers, the vacuum spacing between slabs being 14 a.u. Only Si atoms on one surface (upon which AM adsorbates are placed) were placed in reconstructed positions; the dangling bonds on the bottom surface were saturated by hydrogen atoms.

The plane-wave (PW) basis set used for a 2×1 cell consisted of ~ 550 – 1150 PW's corresponding to an energy cutoff of 4.5–7.5 Ry. For the 2×2 cell we used ~ 1470 PW's corresponding to an energy cutoff of 5.5 Ry. During the self-consistency iterations the charge density was sampled at 15 and 9 \mathbf{k} points, respectively, for the two cells placed uniformly in the surface Brillouin zone (BZ). This parameter set is comparable to the one typically used^{43,45} in electronic-structure calculations for clean Si(001)- 2×1 . The final optimization used 32 \mathbf{k} points and 7.5-Ry energy cutoff in a 2×1 unit cell. We used a very strict SCF convergence criterion (rms deviation in potential $\sim 10^{-7}$) because of the demands⁵⁵ of the calculations of the Hellmann-Feynman forces.

III. RESULTS AND DISCUSSION

A. Structure at $\frac{1}{2}$ a ML ($\Theta=1$) coverage

Our results for the energetics of some binding structures at $\Theta=1$ ($\frac{1}{2}$ ML) for Na/Si were given in a brief rapid communication.²³ They are summarized in Table I for all the sites. The optimization consisted of only moving the AM overlayer along the z direction while the substrate atoms were held fixed at the positions given by the Abraham-Batra⁴⁴ symmetric dimer model. An important point to note is that both H and B adsorption sites have nearly the same total (and hence adsorption) energies. The B site appears to be slightly more favorable (~ 0.01 eV/cell) than the H site when the energy cutoff is increased to 6.5 Ry. However, the difference is too small and does not warrant a clear choice between the H and B sites. At this point a judicious conclusion would be that at room temperature both H and B sites shall be occupied, governed only by the kinetics considerations. We shall be able to give a more definitive conclusion in Sec.

III C upon including the lattice relaxation. The occupancy of C site is found to be somewhat unfavorable at $\frac{1}{2}$ ML but the D and T sites can be clearly ruled out. Also from the last two columns it is clear that reverting to an ideal surface at this coverage is energetically unfavorable. Although the bonding on the ideal surface is actually more favorable, the loss in energy due to dimer breaking (~ 1.6 eV) is not offset by this additional bonding.

In Fig. 2 we have given plots of total energy versus vertical height of the AM overlayer at various sites at $\Theta=1$ for Na/Si. Similar results were obtained for the K/Si system. All energies are referenced with respect to energy of the most stable configuration at the H site and are computed using a 4.5-Ry energy cutoff. The shape of the energy curve around the minimum offers a hint that the H and B sites would be differentially affected upon lattice relaxation. The energy sequence (in the order of decreasing stability), $E(H) \simeq E(B) < E(C) < E(D) < E(T)$, convinces us that the D and T sites can be safely ruled out at this coverage. It thus emerges that the H and B sites are competitive adsorption sites with the C site being a close third at $\Theta=1$. This is true in the absence of lattice relaxation because so far we have held the substrate atoms in fixed positions given by the AB symmetric dimer model.⁴⁴

B. The Δx and Δy Peierls distortions

Ling *et al.*²⁴ have carried out extensive cluster-model calculations for the K/Si system within the framework of local-density total energy formalism using the Hedin-Lundqvist form of exchange-correlation potential. They employed a frozen core approximation and in the spirit of the discrete variational method, represented matrix elements numerically on a three-dimensional grid of points. For the H site at $\Theta=1$, they obtained a K—Si bond length of about 3.2 Å in good agreement with experiment¹² but longer than our value of 2.6 Å. The Si—K interatomic distance might be underestimated in our calculations¹⁸ due to the particular form of the ionic pseudopotential and possibly due also to the form of the exchange-correlation potential. Furthermore, they found a strong (binding energy ~ 3 eV) ionic bond ($\Delta Q \sim 0.63e$ from K to Si). These findings do not lend support to the experimental conclusion⁵⁶ that the alkali-metal—Si bonding is weak and covalent.

Ling *et al.*²⁴ made another important contribution in

TABLE I. Calculated relative energies (in eV) measured with respect to the H site for various adsorption sites for Na at $\Theta=1$ on Si(001)- 2×1 and ideal (I) Si(001) surfaces. The optimized vertical heights h and nearest-neighbor Si—Na interatomic distance d are given in Å. Positive values for ΔE correspond to energetically less favorable configurations. The Bloch states were represented by a basis set of ~ 550 plane waves corresponding to $|\mathbf{k} + \mathbf{G}|^2 < 4.5$ Ry. The numbers in parentheses are for calculations performed with ~ 1000 plane waves, $|\mathbf{k} + \mathbf{G}|^2 < 6.5$ Ry.

Sites	H	B	C	D	T	$I(H)$	$I(B)$
ΔE	0.0	0.03(−0.01)	0.14(0.14)	0.60	0.78	0.89	1.32
h	1.27(1.32)	−0.16(−0.29)	0.64(0.58)	2.27	2.49	0.79	1.80
d	2.60(2.62)	2.64(2.66)	2.83(2.79)	2.57	2.49	2.83	2.63

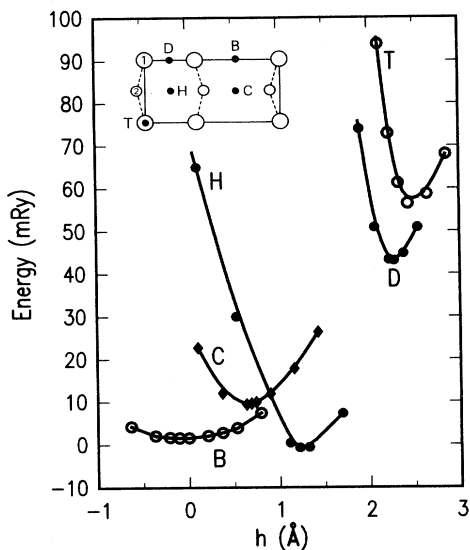


FIG. 2. Total energy as a function of the vertical height h of the alkali-metal overlayer above the Si(001)-2×1 surface at various adsorption sites shown in the inset. Substrate atoms were held in fixed positions given by the Abraham-Batra (Ref. 44) symmetric dimer model. All energies are referenced with respect to the most stable H site.

their search for the optimum site. They found that the adsorption at the H site is unstable to a zigzag Δx distortion of K atoms shown in Fig. 1(b). The resulting lowering of energy upon this Peierls's type of distortion they obtained is redrawn in Fig. 3 by dashed lines. Here we chose the zero of energy at the maximum distortion $\Delta x \approx 1.6 \text{ \AA}$ computed by Ling *et al.*²⁴ Their computed data points are shown by open circles through which the dashed line has been drawn to guide the eye. The instability of the H site towards such a distortion was used as a clue that a more optimum adsorption site may lie elsewhere. In fact, they concluded that the long bridge site is more stable than the H site.

We also computed total energy at the H site as a function of Δx within our slab model. To carry out the calculations we used the 2×2 periodic cell shown in Fig. 1(b). Our results for the Na overlayer held at a fixed height ($\sim 1.2 \text{ \AA}$) above the Si(001)-2×1 surface are shown in Fig. 3 by the solid line and do not show any instability due to Δx distortion. Results were similar for the K-Si system as inferred from calculations done using only a few Δx values. In view of this lack of agreement with the cluster results, we must examine various sources which might be responsible for the difference. Two points readily come to mind. First of all, our Si—K bond length is short. Secondly, holding the z position of the overlayer fixed is only valid near small $\Delta x \leq 0.5 \text{ \AA}$. Beyond this one should, in principle, reoptimize the vertical position because the AM—Si bond length is no longer optimum. Consequently, we performed calculations for the K overlayer placed above the H sites at a height of about 2 Å. This gave the Si—K bond length equal to the empirical value of 3.1 Å. A Δx distortion of about 0.25 Å still

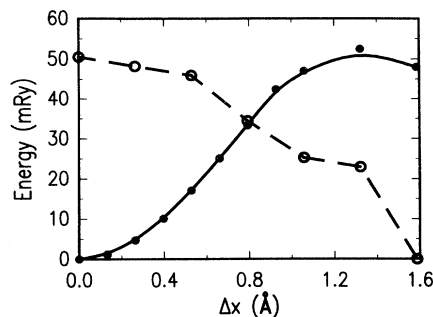


FIG. 3. Total energy as a function of Δx Peierls distortion away from the H site shown in Fig. 1(b). Dashed lines with open circles are Ling *et al.*'s cluster-model results (Ref. 24) for K-Si redrawn here by setting the zero of energy arbitrarily at their highest computed Δx value. Solid lines with dots are our results for Na-Si obtained in a periodic 2×2 cell [Fig. 1(b)] referenced with respect to adsorption at the H site.

raised the total energy with respect to the undistorted structure. The increase in energy is smaller; 1 mRy, as opposed to 4 mRy.

We next examined whether the substrate relaxation in the presence of Δx distortion can lead to a lower energy configuration compared to $\Delta x = 0$. To this end we took the optimized H site geometry in a 2×2 cell with $\Delta x = 0$. Upon introducing $\Delta x \approx 0.5 \text{ \AA}$ we noted an increase of energy by 16 mRy. This was the case when all the other atoms and also the (y, z) coordinates of the AM overlayer were held fixed corresponding to $\Delta x = 0$ calculations. Upon substrate relaxation and reoptimization of the alkali-metal overlayer (y, z) coordinate forces, we recovered 4 mRy. Hence the Δx distortion was still unfavorable by 12 mRy per 2×2 unit cell. This is to be compared with the 17-mRy energy deficit shown in Fig. 3 obtained for fixed atomic positions (of the AB model).

We then considered the effect of the Δx distortion on the total energy in the limit of infinite separation between AM and Si. Such a calculation can be simply done using an unsupported AM overlayer stacked along the y direction. The interatomic Na-Na distance was set at 3.84 Å to correspond to the AM situated on Si(001)-2×1. We found that a $\Delta x = 0.5 \text{ \AA}$ raised the energy by 4.5 mRy. Such a distortion still leaves all interatomic distances uniform but at a value of 3.98 Å. It has been shown⁵⁷ that the Δx motion of AM atoms does not open any energy gaps at the zone edge. Also the space group for the Δx distorted structure is nonsymmorphic and therefore all bands have to be doubly degenerate at one zone boundary. The Fermi level passes through the degeneracy point at the zone edge and the system is intrinsically metallic. Thus the energy lowering mechanism due to a gap opening at the zone edge is not operative²⁴ for the Δx distortion. Clearly the site energies remain degenerate upon Δx distortion. The change in total energy arises from the change in chemical potential. On the other hand, a small $\Delta y = \pm 0.25 \text{ \AA}$ distortion lowered the total energy by 1.1 mRy. The Δy distortion is a dimer-forming distortion which breaks the degeneracy at the zone edge and the energy is lowered due to Peierls mechanism. For the AM

overlayer adsorbed at the H sites any sizable Δy distortion is precluded due to the presence of surface Si atoms. Whether or not the Δx distortion in the presence of substrate lowers the total energy is predominantly governed⁵⁷ by the AM-Si interactions.

The energy lowering upon Δx distortion found by Ling *et al.*²⁴ may have its origin in some cluster artifacts. It is also unexpected that their energy continues to decrease monotonically even for large Δx which places the K atom at the edge of the cluster. It is possible to lower the total energy upon bond optimization without opening the gap at E_F . This can be seen by replacing monovalent alkali metal atoms with the trivalent metal atoms like Al in the 2×2 cell shown in Fig. 1(b). The total energy as a function of Δx is given in Fig. 4. The lowering in energy is brought about by bond optimization because both the distorted and undistorted structures are metallic.⁴⁶ Also a minimum in energy is seen as a function of Δx which is a signature of the optimum bond. It is possible that the absence of a minimum in the cluster calculations²⁴ is also a cluster artifact.

The absence of Δx distortion for AM in our calculations is due to resultant unfavorable bonding. Since the alkali metal is in a more or less ionized state, the Δx distortion amounts to essentially moving bare AM ions towards Si. This tends to raise the energy since, as discussed above, the Δx distortion does not open a gap at E_F . Thus in our calculations the bond is optimal at the H site without any distortion.

The Δy type of Peierls distorted structure at the B sites shown in Fig. 1(c) offers another adsorption geometry at $\Theta=1$. This corresponds to the dimerization of Na at the B sites and has been observed⁴⁷ for Ga adsorption on Si(001). For AM we found such a dimerization to be energetically unfavorable. The origin of this is traced to the fact that AM atoms are in a more or less ionized state on the surface. Bringing the ionized atoms towards each other does not create any bonding interaction and hence the energy is raised. Thus the AM dimerization (Δy distortion) at the B site is also ruled out. It is surprising that Ling *et al.*²⁴ again find a small Δx distortion at the B sites.

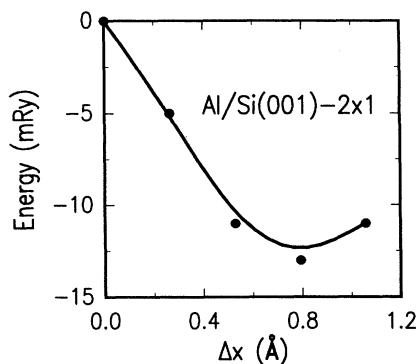


FIG. 4. Total energy as a function of Δx Peierls distortion away from the H site for Al-Si obtained in a periodic 2×2 cell [Fig. 1(b)] referenced with respect to adsorption at the H site.

In closing this subsection, we emphasize that in our slab model calculations the Δx distortion of the H sites and Δy distortion of the B sites are energetically unfavorable. Thus both the H and B sites are competitive overlayer adsorption sites in the absence of the substrate relaxation which we now address.

C. Lattice relaxation

It emerges that the H and B sites are important sites at $\Theta=1$ and are also consistent with the observed 2×1 LEED patterns. Now we include the substrate relaxation. Complete relaxation calculations are carried out for the Si-Na system; similar relaxations are expected for Si-K. So far we have held the substrate atoms in fixed positions given by the AB symmetric dimer model.⁴⁴ Therefore we calculated the Hellmann-Feynman forces acting on various atoms. Each Si plane, n , has two atoms in the 2×1 unit cell labeled n and n' . In Table II, F_x and F_z components of forces (in units of 10^{-8} N ≈ 0.25 Ry/a.u.) acting on the eight Si atoms in the top four planes are given. For the calculational parameters at hand forces less than or equal to 0.05×10^{-8} N are to be considered small. The y components of forces were always negligibly small. We note that for Na in the optimized position, significant forces are present on the first and third layer Si atoms in the AB model. The direction of forces on the top layer Si atoms (1 and 1') is such that the dimer bond "wants" to shrink somewhat and the layer as a whole "wants" to relax inwards. Since there are also significant forces on the third layer Si atoms (3 and 3') suggesting buckling, we felt that these forces must be intrinsic to the AB model for the substrate itself.

Consequently, we used a more recent symmetric dimer model optimized by Batra.⁴⁵ This model is similar to the Yin-Cohen model⁴³ as far as subsurface atoms are concerned but is symmetric. It has buckling in the third and

TABLE II. Forces (in units of 10^{-8} N) on the top four layers of Si atoms in the presence of the Na overlayer adsorbed at the H site. Atomic positions (in a.u.) for Si's are from the Abraham-Batra symmetric dimer model (Ref. 44) but the vertical height has been optimized here. Forces were computed using the 2×1 cell. No significant y forces ($F_y=0$) were detected. The Bloch states were represented by a basis set of ~ 730 plane waves corresponding to $|\mathbf{k}+\mathbf{G}|^2 < 5.5$ Ry and 15 k points in the Brillouin zone.

N	x	y	z	F_x	F_z
Na	0.0	3.63	2.30	0.0	-0.003
1	-2.27	0.0	-0.19	0.049	-0.143
1'	2.27	0.0	-0.19	-0.049	-0.143
2	-3.43	3.63	-2.53	-0.023	0.044
2'	3.43	3.36	-2.53	0.023	0.044
3	0.0	3.63	-5.13	0.0	-0.186
3'	7.26	3.63	-5.13	0.0	0.163
4	0.0	0.0	-7.70	0.0	-0.007
4'	7.26	0.0	-7.70	0.0	0.018

also in the fourth layer. Other important differences between this and the AB model are (i) shorter (4.12 versus 4.54 a.u.) dimer bond length and (ii) smaller (1.9 versus 2.3 a.u.) interlayer spacing between first and second Si layers. The optimized Na position and the forces on various atoms on Batra's symmetric dimer model⁴⁵ of the surface are presented in Table III. Comparing with the Table II values, we note that $d(\text{Si}-\text{Na})$ is unchanged at ≈ 4.9 a.u. and the forces on the third layer Si atoms are drastically reduced. These forces must then be intrinsic to the AB model⁴⁴ itself and not due to the influence of the overlayer.

Next we moved various atoms in the direction of the forces and obtained an optimized structure given in Table IV. It turns out that forces on different atoms are strongly correlated. Thus when we stretched the dimer bond to what we believed to be the optimum value of 4.38 a.u., we noted strongly opposing forces on first and second layer Si atoms trying to push them apart. These forces were relieved by relaxing the top layer Si outwards (along the z direction) by 0.22 a.u. and moving the second layer Si atoms towards each other by a small amount, namely, ± 0.05 a.u. The Na overlayer then settled at a slightly higher z value to attain $d(\text{Si}-\text{Na})$ which is remarkably constant (4.9 a.u.) for all the substrate models investigated here.

Thus the major relaxation introduced in the lattice (with respect to Batra's symmetric dimer model) due to the presence of the Na overlayer at the H sites is to increase the Si dimer bond length towards bulk value. Recall that Batra's dimer bond length at the surface is 4.1–4.2 a.u., which increases at 4.38 a.u. in the presence of the Na overlayer. The bulk value is 4.44 a.u. (if one were to compare with respect to the AB model then the dimer bond length has been reduced from 4.54 to 4.38 a.u.) The interlayer spacing between the first and second layer Si is increased from 1.89 to 2.11 a.u. but is still below the bulk value of 2.56 a.u. The direction of relaxations towards bulk values is physically reasonable because the AM overlayer supplies some charge to the dangling

TABLE III. Initial atomic coordinates (in a.u.) for the top four surface layers for the Si(001) 2×1 symmetric dimer model by Batra (Ref. 45) used in optimizing the Na vertical height above the surface. Forces (in units of 10^{-8} N) for the Si's in the top four layers and on Na are given. Forces were computed using the 2×2 cell with 5.5-Ry cutoff and 9 k points in the BZ. No significant y forces ($F_y=0$) were detected.

N	x	y	z	F_x	F_z
Na(H)	0.0	3.63	1.80	0.0	-0.001
1	-2.06	0.0	-0.84	-0.215	0.029
1'	2.06	0.0	-0.84	0.215	0.029
2	-3.45	3.63	-2.73	0.032	-0.086
2'	3.45	3.63	-2.73	-0.032	-0.086
3	0.0	3.63	-5.51	0.0	-0.002
3'	7.26	3.63	-5.05	0.0	0.031
4	0.0	0.0	-7.89	0.0	0.003
4'	7.26	0.0	-7.63	0.0	-0.017

bonds. To the dangling bonds it appears as though there is another layer of Si present and there is an attempt to continue the Si lattice. Hence the relaxation in the direction of the bulk.

We also carried out optimizations at B and C sites. The most significant finding is the energy sequence: $E(H) < E(B) < E(C)$. The B and C sites are less stable than the H site by 0.15 and 0.25 eV, respectively. These values changed to 0.12 and 0.22 eV upon increasing the energy cutoff to 7.5 Ry. The distinction between H and B sites is much sharper, unlike the results shown in Fig. 2 for the fixed lattice given by AB.⁴⁴ This has been brought about by the preferential lowering of the energy at the H site relative to the B site upon lattice relaxation. Since the energy function at the B site in Fig. 2 is rather flat, one does not expect much change upon relaxation. The H site can and does benefit more upon relaxation. The C site also benefits more than the B site but since it had higher energy to start with it continues to be less stable. A physical argument in favor of the H site over B and C sites can be constructed. Since AM atoms are fairly electropositive they can be well screened from each other at the H sites by the intervening electronic charge in the dangling bonds. Such a screening is much less effective at the B and C sites. Our computed $d(\text{Si}-\text{Na})$ are 2.60, 2.75, and 2.83 Å at H , B , and C sites, respectively. These values have not changed¹⁰ much upon optimization. Similar relaxations are expected for the Si-K system.

We finally optimized atomic coordinates at H and B sites using an extended basis set, namely, 7.5-Ry energy cutoff and 32- k points in the Brillouin zone. These results are given in Table V. An extensive LEED calculation⁵⁸ has concluded that at $\frac{1}{2}$ ML coverage best agreement with data is obtained for the Na overlayer adsorbed at the H sites at a vertical distance of 1.85 Å. In fact, the two structures with relatively low Pendry R factor (averaged over several beams) values of 0.25 and 0.33 both involve adsorption at the H sites but with different vertical heights of the Na overlayer of 1.85 and 1.25 Å, respectively. Based on the R -factor value of the structural model with $h=1.85$ Å was selected as optimum. Our

TABLE IV. Optimized atomic coordinates and the residual forces acting on various atoms. Forces (in units of 10^{-8} N) for the Si's in the top four layers and on Na are given. Forces were computed using the 2×2 cell with 5.5-Ry cutoff and 9 k points in the BZ. No significant y forces ($F_y=0$) were detected.

N	x	y	z	F_x	F_z
Na(H)	0.0	3.63	1.85	0.0	0.005
1	-2.19	0.0	-0.62	0.012	-0.032
1'	2.19	0.0	-0.62	-0.012	-0.032
2	-3.40	3.63	-2.73	0.028	-0.026
2'	3.40	3.63	-2.73	-0.028	-0.026
3	0.0	3.63	-5.51	0.0	0.004
3'	7.26	3.63	-5.05	0.0	0.049
4	0.0	0.0	-7.89	0.0	-0.002
4'	7.26	0.0	-7.63	0.0	-0.014

TABLE V. Optimized atomic coordinates for Na at H and B sites and the corresponding top two Si layers in the 2×1 cell. Atomic coordinates for other layers are the same as in Table IV. These calculations were performed with 7.5-Ry cutoff and 32 k points in the BZ. No significant y forces ($F_y=0$) were detected.

N	x	y	z	F_x	F_z
Na(H)	0.0	3.63	1.85	0.0	0.008
1	-2.19	0.0	-0.65	-0.001	-0.019
1'	2.19	0.0	-0.65	0.001	-0.019
2	-3.40	3.63	-2.73	-0.010	-0.025
2'	3.40	3.63	-2.73	0.010	-0.025
Na(B)	7.26	0.0	0.40	0.0	-0.032
1	-2.19	0.0	-0.50	-0.024	0.043
1'	2.19	0.0	-0.50	0.024	0.043
2	-3.40	3.63	-2.73	0.019	0.005
2'	3.40	3.63	-2.73	-0.019	0.005

computed distance in Table V at the H site is somewhat smaller ($\sim 1.3 \text{ \AA}$).

The B adsorption site has been favored by the calculations of Ling *et al.*²⁴ and Ramirez²⁵ with K—Si bond lengths of 3.2 and 2.65 \AA , respectively. Although we find the B site to be somewhat less stable for Na—Si our value of $d(\text{Na—Si})$ lies in this range and is 2.75 \AA . All these bond-length values imply a shorter vertical height of the AM overlayer above the Si surface relative to the H site adsorption. In other words, a similar value of the bond length at the H site shall place the AM overlayer at a higher vertical distance. It appears to us that these short vertical heights at B sites are not likely to produce sufficient change in the normal dipole moment. Thus the large work-function lowering which is often observed at semiconductor surfaces may be difficult to explain by the B site adsorption. This has been independently confirmed by other calculations.⁵⁹ Furthermore, if AM's are adsorbed on the B sites, one has yet to explain how Si(001) is activated⁶⁰ to NEA since B sites are not available for oxygen adsorption. Recall that the NEA has been explained³³ on the basis of the H site occupancy by AM followed by B site occupancy by oxygen atoms. These difficulties are not present if AM's are adsorbed at the H site as indicated by our calculations.

A recent STM datum has been interpreted⁴⁰ in terms of adsorption at the T site at very low ($\lesssim 0.1$ ML) AM coverages. The lowest coverage used in our work is $\frac{1}{2}$ a ML and as such a direct comparison is not possible. However, some significant conclusions can be drawn by examining the calculated Hellmann-Feynman forces. The forces on various atoms in the optimized (with respect to the vertical height h of the AM overlayer) structure at the T site (see Fig. 2) on a symmetric dimer model⁴⁴ showed an asymmetric pattern. The dimer-forming surface Si atom in the 2×1 cell, which did not have the Na atom located above it, "felt" a large force of 0.2×10^{-8} N along the $-z$ direction suggesting an asymmetric buckling of the surface. We therefore placed the AM overlayer above the T site on the Yin-Cohen⁴³ asymmetric Si(001)- 2×1 (as

modified by Batra⁴⁵) substrate. This lowered the total energy by about 14 mRy with respect to the value shown in Fig. 2. Another 15-mRy stabilization was achieved upon including complete substrate relaxation (most of which was due to stretching the surface dimer bond towards the bulk value of about 4.4 a.u.). Thus nearly 30 mRy has been gained with respect to the value shown for the T site in Fig. 2. But it is still less stable than the H and B sites (even in the absence of substrate relaxation) shown in Fig. 2. Thus it is clear that at $\frac{1}{2}$ a ML, the T site is not the most stable site. However, as proposed by Hashizume *et al.*,⁴⁰ an asymmetric buckling is definitely stabilized if and when the T site is occupied.

According to our calculations^{18,23} an AM overlayer partly fills the dangling bond band leading to a metallic state. Since STM is sensitive to charge density at E_F , it is conceivable that the surface dangling bonds are being imaged by the experiment.⁴⁰ This might give the impression of the T site occupancy. However, if an H site were to be occupied at the lowest coverage one should see four surrounding Si atoms. Since only one site is imaged by the experiment⁴⁰ we can speculate that the adsorption site at the low coverage is evidently different from what we have found at $\frac{1}{2}$ a ML coverage. If at low coverage the T site is occupied, then our calculation also supports the stabilization of the asymmetric dimerization postulated by Hashizume *et al.*⁴⁰ It has been shown⁴⁸ for In on Si(001) that the coordination number of In is 3 for very low coverages and 2 for $\frac{1}{2}$ ML coverage. Coverage-dependent changes are possible for AM's also because at $\frac{1}{3}$ ML coverage either a mixed site model^{23,24} or a major reconstruction of the lattice has to be postulated¹³ to explain the LEED data. This is discussed at length in Sec. III F.

The binding energy E_b of the adsorbed AM overlayer at the H site,

$$E_b = E_T[\text{Si} + \text{AM}] - E_T[\text{Si}] - E_T[\text{AM}],$$

is obtained from the total energies of the Si + AM system, the bare substrate (Si) and the overlayer (AM) all calculated using slabs of the same dimensions. A negative value for E_b corresponds to a stable bonding arrangement for the overlayer. The calculated binding energy is $E_b = -2.5$ eV per Na in the 2×1 cell for the AB model of the substrate given in Table II. The binding energy is reduced to 2.15 eV if the substrate coordinates optimized by Batra⁴⁵ and given in Table III are used. The completely optimized structure discussed in Table IV gives $E_b = -2.23$ eV. The more stable E_b in the AB model is primarily due to the higher reference substrate energy than the optimized substrate energy. These energies, however, should not be directly compared with the desorption energy of single Na atom since we are desorbing the overlayer as a whole. Our computed values have a deficit of an amount equal to the cohesion in the overlayer. On the other hand, the local-density approximation overestimates bonding energies. Hence the absolute energies should be viewed with caution. But in agreement with Ling *et al.*,²⁴ we conclude that the AM-Si bonding is strong.

D. Electronic structure and ionicity

In Fig. 5 we show the band structure for the 2×2 cells for clean and Na covered surfaces since the optimization was done in these large cells. The \bar{J}' states have been folded back to the $\bar{\Gamma}$ point due to doubling of the period along the [110] direction. The zone edge along this direction is labeled as \bar{J}_1 which lies at the midpoint between $\bar{\Gamma}$ and \bar{J}' . No new bands due to Na(3s) are present around E_F . We note the partial filling of the dangling bond states by Na(3s) electrons from the movement of the Fermi level.

Values for the charge transfer, ΔQ , from AM to Si have ranged from 0 to ~ 1 in the literature.^{7,12,18–25,59} It has been shown earlier^{18,23} by us that the AM charge is localized in the region between the AM overlayer and the top Si surface layer. The problem, however, lies in uniquely assigning this charge to a particular center. Hence the amount of covalency or ionicity in the bond cannot be quantitatively stated with much confidence. At least, we have not found a recipe for doing so satisfactorily. We can produce almost any value for ΔQ between 0 and 1 depending upon the way we partition the space. Couple this with the uncertainty in the precise vertical height of the AM overlayer and it becomes clear that space partitioning is not the choice method for projecting ΔQ . However, an examination of the spatial²³ and spectral distribution of the charge density (see Fig. 5) leads to the conclusion that there is significant charge transfer from Na to Si. The absence of any Na(3s) related bands below E_F further suggests that metallicity has its origin in the partial occupancy of surface dangling bonds. We find no evidence for the AM overlayer chain itself being metallic at $\Theta=1$.

In Fig. 6, the computed constant energy contour ($E=E_F$) in one quadrant of the surface Brillouin zone is at $\Theta=1$ for the *H* site. A fine mesh in *k* space was employed for these calculations. The metallicity is due to the Fermi line crossing the dangling bond band. The

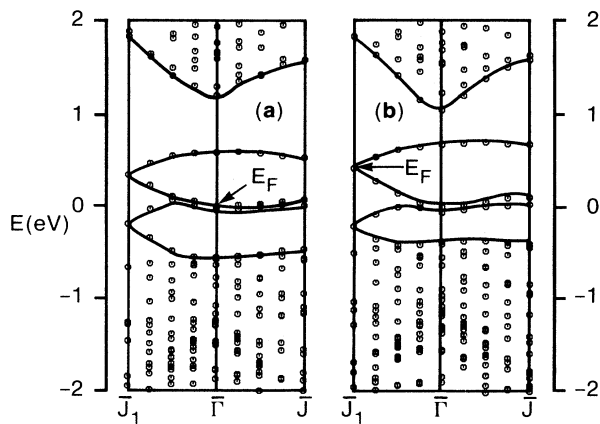


FIG. 5. Band structure for (a) Si(001)-2×1 calculated using a 2×2 cell. The doubled periodicity along the *y* direction folds \bar{J}' onto $\bar{\Gamma}$. The edge of the zone thus occurs at the midpoint \bar{J}_1 . (b) Electronic structure for Na-covered Si(001)-2×1 at $\Theta=1$ using a 2×2 cell. The major change from (a) is the shift of E_F .

upper half of the zone is occupied by electrons at $T=0$ K. By extending the “Fermi surface” to the first Brillouin zone using the fourfold symmetry, we at once note that the Fermi surface is not completely nested. Thus the *H* site is expected to be stable against any Δx of Δy type of Peierls distortion. This was indeed found in Sec. III B from detailed total energy calculations.

E. Structure at 1 ML ($\Theta=2$) coverage

We briefly present the results of our theoretical calculations at $\Theta=2$ (1 ML). A plausible structure^{23,25} at $\Theta=2$ involves occupying the *H* and *B* sites simultaneously. An alternative involves occupying the *H* and *C* sites simultaneously.^{9,10} Simultaneous occupation of *B* and *C* sites can be ruled out on physical grounds. For a fixed lattice model⁴⁴ given by AB,⁴⁴ the (*H-C*) structure was found²³ to be less favorable by about 0.1 eV per unit cell.

Here we allowed lattice relaxation and reoptimized the (*H-B*) and the (*H-C*) structures. The resultant structures described in Table VI cannot be distinguished⁵⁹ based on our total energies. The AM overlayer attempts to lift the 2×1 reconstruction. This is evident from the Si dimer bond length which is being stretched beyond its value at the surface (4.2 a.u.) as well as the bulk value (4.4 a.u.). The stretching of the dimer bond is due to charge transfer from AM to antibonding Si surface bands. The stretch offers a depolarization mechanism as more charge is transferred from AM to dangling bonds at $\Theta=2$. The AM overlayer does not succeed in fully lifting the reconstruction because we find²³ that reverting to an ideal surface is energetically unfavorable (by ≥ 0.6 eV) at monolayer AM coverage. For comparison, the 2×1 reconstruction is lifted^{46,48} by Al and Ga at about $\frac{1}{2}$ ML coverage. Both the (*H-B*) and (*H-C*) structures obtained by us are puckered, with $\Delta h \approx 0.7-0.9$ Å. A puckered structure at monolayer coverage of K on Si(001)-2×1 has been proposed¹⁰ with $\Delta h \approx 1.1$ Å.

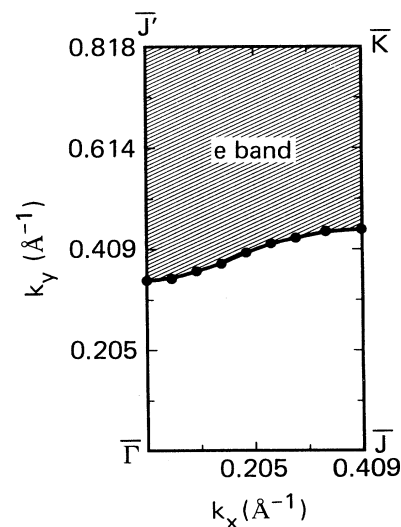


FIG. 6. The constant energy contour $E=E_F$, shown by solid dots, in one quadrant of the surface Brillouin zone for Na/Si(001)-2×1 at $\frac{1}{2}$ ML coverage. The shaded area shows the occupied electron band.

TABLE VI. Optimized atomic coordinates (in a.u.) and the residual forces (in units of 10^{-8} N) on various atoms for Na-Si(001)- 2×1 at $\Theta=2$ for the (*H-B*) and the (*H-C*) adsorption models. These calculations were performed with 6.5-Ry cutoff and 15 *k* points in the BZ. No significant *y* forces ($F_y=0$) were detected. Atomic coordinates for the other layers are those given in Table IV.

<i>N</i>	<i>x</i>	<i>y</i>	<i>z</i>	F_x	F_z
Na(<i>H</i>)	0.0	3.63	2.38	0.0	-0.014
Na(<i>B</i>)	7.26	0.0	0.67	0.0	-0.13
1	-2.35	0.0	-0.25	-0.002	-0.022
1'	2.35	0.0	-0.25	0.002	-0.022
2	-3.33	3.63	-2.73	0.024	0.012
2'	3.33	3.63	-2.73	-0.024	0.012
Na(<i>H</i>)	0.0	3.63	2.40	0.0	-0.031
Na(<i>C</i>)	7.26	0.0	1.10	0.0	-0.027
1	-2.50	0.0	-0.25	-0.012	0.016
1'	2.50	0.0	-0.25	0.012	0.016
2	-3.33	3.63	-2.73	0.004	-0.008
2'	3.33	3.63	-2.73	-0.004	-0.008

Our calculated electronic structure at $\Theta=2$ is rather similar to that shown in Fig. 5. At $\Theta=1$, a single alkali-metal adsorbate atom per unit cell partly filled the upper dangling band leading to a metallic state. At $\Theta=2$, the 2×1 unit cell has just enough electrons to fully occupy all dangling bond bands leading to a semiconducting⁹ surface. An important point is that the AM overlayers do not introduce any new bands around E_F even at $\Theta=2$. The reentrant behavior to the insulating state¹⁵ as a function of coverage thus follows naturally from our calculations. The origin of the above metal-insulator transition is traced to the ionic interaction between the alkali metal and Si, and to the presence of active surface states on the Si surface.

A recent⁹ angle-resolved ultraviolet photoemission spectroscopy study for a single-domain Si(001) 2×1 -K has been presented. Earlier experiments were done on double-domain Si(001)- 2×1 from which it is difficult to obtain dispersion of surface states in an unambiguous fashion. Single-domain Si(001)- 2×1 was obtained by growing epitaxial Si layers onto a Si wafer held at 500°C and then annealing it at 1000°C. Potassium was then deposited on this substrate held at room temperature under a pressure of $\sim 6\times 10^{-10}$ to obtain K-saturated single-domain Si(001)- 2×1 . Two filled surface state bands, D_1 and D_2 , were indeed detected with ARUPS and their measured dispersion is reproduced in Fig. 7. In agreement with our above conclusion for $\Theta=2$, no additional bands directly attributable to K(4*s*) were found and the surface was indeed semiconducting.

Our calculated dispersions for the surface bands are shown in Fig. 7 for *H-B* as well as *H-C* site occupancies by K. In view of some uncertainty in our computed $d(\text{Si-K})$ values, we have also shown results by placing dilayer at empirical height. The empirical K heights above the surface at *H-B* sites were obtained by fixing $d(\text{Si-K})=3.1$ Å for both *H* and *B* sites. This then led to $h_1=2.1$ Å (height above the *H* site) and $h_2=1.5$ Å

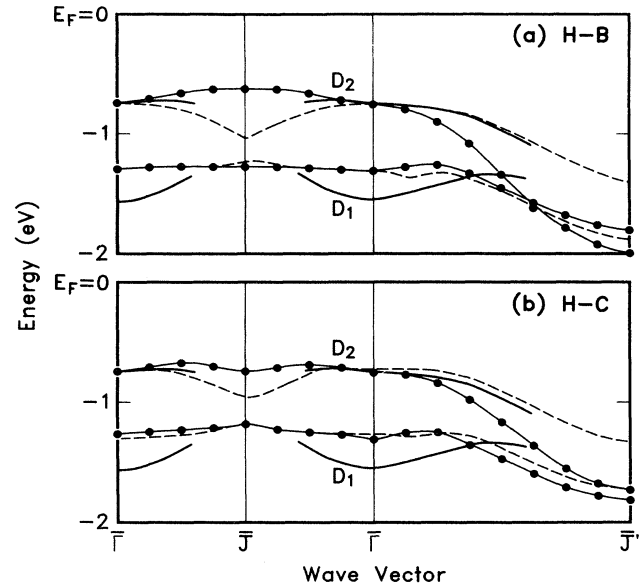


FIG. 7. Comparison of calculated electronic structure for K-Si at $\Theta=2$ with ARUPS data. Solid lines with dots are our results for K atoms at optimized positions above the Si surface. Dashed lines give dispersions computed for K placed at empirical heights. Results for the *H-B* and *H-C* models are shown in panels (a) and (b), respectively. ARUPS data around E_F on a single domain Si(001)- 2×1 dosed to saturation with K is shown by solid lines in both the panels. It is reproduced from the work of Enta *et al.* (Ref. 9).

(height above the *B* site). These vertical heights were also used for calculations at *H-C* sites. The K dilayer is thus puckered by the same amount for *H-B* and *H-C* calculations. In all cases we set the energy of the D_2 band at the center of the Brillouin zone to coincide with the measured value. The shape, location, and dispersion of the lower-lying D_1 band is essentially independent of sites and vertical positions of K atoms. This band can be brought in better registry with the measured data by a 0.5-eV shift downwards. Thus this band does not provide much help in deciding among various possibilities. The measured D_2 band is well described in terms of *H-B* sites for K's at empirical distances but only moderately less well by *H-C* occupancies. In view of the fact that one-electron eigenvalues from Kohn-Sham equations are not precisely comparable to the measured band in ARUPS, we cannot really make a definitive choice. However, there is no doubt that both *H-B* and *H-C* lead to a semiconducting surface and support a picture of substrate metallization at coverages below saturation.

We also examined the dispersion of bands around E_F for fully optimized Na/Si structures at (*H-B*) and (*H-C*) sites. Results are quite similar to those described above for K-Si with one exception. At the \bar{J} point the two dangling bond derived bands become nearly degenerate for the (*H-C*) model but not for the (*H-B*) model.

F. Third-order ($\Theta = \frac{2}{3}$) structure

A third-order structure has been reported^{13,34} for Na, K, and Cs adsorption on Si(001) but no satisfactory mod-

el exists so far. Holtom and Gundry³⁴ observed the 2×3 structure at coverages $\frac{1}{3} \leq \Theta \leq \frac{2}{3}$. They suggested that the low coverage 2×3 structure is due to Cs atoms at every fourth H site along the y direction (see Fig. 1). Since the intensity of the $(\frac{1}{3}, 0)$ spot grew at the expense of the $(\frac{2}{3}, 0)$ spot with increasing coverage, they placed additional Cs atoms at the middle positions along the y direction. This corresponds to placing the additional Cs atom at an adjacent short bridge site D (above the center of the Si dimer) next to an H site. The unit cell is 2×3 , with one Cs atom at H and another one at D , for a coverage of $\Theta = \frac{2}{3}$. If one looked at the overlayer alone (ignoring substrate altogether) it has the periodicity of 2×1.5 . Such a unit cell does not give any primary third-order spots. In practice, because of the substrate, the overall periodicity is 2×3 and hence $(\frac{1}{3}, 0)$ spots shall be present but with reduced intensity. Thus with this mixed site occupancy model, Holtom and Gundry successfully accounted for the LEED data. Batra²³ presented a slight variation of this model by noting that the H and B sites have nearly identical adsorption energies. Hence he suggested that the dimer bridge site D , invoked by Holtom and Gundry,³⁴ ought to be replaced by B . Reduced intensity of the third-order spots in our model follows from the fact that alkali-metal atoms at H and B sites have different vertical heights above the surface.

Glander and Webb¹³ have argued that none of the above mixed site models can account for their observations of the third-order structure for Na-Si(001). In particular, a drastic decrease of the intensity of the half-order beams led to a proposal of a major reconstruction of the Si substrate for the third-order structure. This consisted of removing every third surface Si atom along the x direction and allowing the second layer atoms beneath them to dimerize by appropriate $\pm \Delta y$ movements. The dimers at the surface are now separated by 3 along the x direction while the second layer dimers are separated by 2 along the y direction. Such a reconstruction clearly reduces the intensity of the half-order spots because the "2"-periodicity is only due to dimers in the second Si layers. Furthermore, there is only one such dimer per 3×2 cell as compared to three dimers in the 2×3 cell involved in the mixed site models. Another nice feature of the reconstruction model is that it can continuously go to the 2×1 structure at $\frac{1}{2}$ ML by only filling the H sites. It is important to note that the proposed¹³ reconstruction cannot produce a 2×3 periodicity (only 3×2) and a mass transport is required. Furthermore, there is no other independent evidence yet for any major structural rearrangement in the substrate brought on due to the adsorption of alkali metals. The proposed reconstruction has eliminated the three surface B sites and replaced them by a single buried B site. Since there are indications that the B site is also a preferred site (in addition to the H site) the reconstruction model may lead to an energy-deficit structure.

The competitive filling of the B sites suggests that our model²³ of the 2×3 structure requires some further discussion. At $\Theta = \frac{1}{3}$, the third-order structure can have adsorbates at either H or B sites as long as every fourth

such site is occupied along the y direction. With increasing coverage both sites must be occupied. An adsorbate in an H site blocks off four surface sites. Then the next alkali-metal atom can adsorb in a B site, but must skip the adjacent 2×1 cell. This gives rise to a 2×3 structure at $\Theta = \frac{2}{3}$ ($\frac{1}{3}$ ML coverage). The reduced intensity of $(\frac{1}{3}, 0)$ and $(\frac{2}{3}, 0)$ spots arises from puckering or different vertical adsorption heights at the two sites. The mixed site models have one additional constraint. They can produce a 2×1 structure (at $\frac{1}{2}$ ML) as a function of increasing coverage only if there is sufficient energy available for diffusion. Remember in the mixed site model we are occupying both H and B sites but for the 2×1 periodicity the same symmetry sites must be occupied in all cells. For this to happen, alkali-metal atoms must be able to move around. At monolayer coverage all H and B sites can be filled and we again recover a 2×1 structure.

It might be argued that since the B site is a viable adsorption site why not explain the entire coverage range with the B site occupancy. In this case the 2×3 structure shall arise by filling every fourth B site. But then the mechanism of skipping two B sites remains unexplained. Also, this opens up the question of how Si(001) is activated to the negative-electron-affinity state. Recall that the NEA has been explained³³ on the basis of the H site occupancy. In any case this is a subject that ought to be explored further.

IV. CONCLUSION

We conclude from our calculations that at the lower coverage, the quasihexagonal site proposed by Levine³³ and a long bridge site along the dimerization direction are equally favorable in energy in the absence of lattice relaxation. The discrimination between the two sites is sharper when the underlying lattice is relaxed making the H site more favorable. A fully optimized model at the quasihexagonal adsorption site shows small lattice relaxation due to the presence of the AM overlayer. We do not find any Δx or Δy distortion instability of the H adsorption sites. To pursue bond optimization, results for Δx distortion for Al on Si(001) are given. The top site is found to be energetically least favorable at $\frac{1}{2}$ a ML coverage. However, if the T site is occupied at very low coverages as indicated by STM experiments then an asymmetric buckling of the substrate is indeed stabilized. A critical evaluation of the 2×3 structure has revealed that further work is necessary to establish a structural model. At the monolayer coverage ($\Theta = 2$), the structure we find is puckered in accord with recent experiments. We also compare our calculated electronic structure with the recent ARUPS data on single domain Si(001)- 2×1 . The surface is metallic at $\Theta = 1$ and semiconducting at $\Theta = 2$. The 2×1 reconstruction of Si(001) is shown to be stable up to 1 ML coverage of AM although the dimer bond is stretched. This is contrasted with metals like Al which lift the surface reconstruction at about $\frac{1}{2}$ ML coverage.

ACKNOWLEDGMENTS

I wish to acknowledge useful discussions with Professor D. J. Scalapino and Dr. Shoucheng Zhang, who have taught me about the various aspects of the Peierls transition.

- ¹R. U. Martinelli, Appl. Phys. Lett. **16**, 261 (1970).
- ²R. U. Martinelli and D. G. Fisher, Proc. IEEE **62**, 1339 (1974).
- ³See, for example, B. Hellsing, Phys. Rev. B **40**, 3855 (1989).
- ⁴For a number of important articles see *Proceedings of the NATO Advanced Res. Workshop on Metallization and Metal-Semiconductor Interfaces, Garching, 1988*, edited by I. P. Batra (Plenum, New York, 1989), Vol. 195.
- ⁵H. Tochiyama, Surf. Sci. **126**, 523 (1983); T. Aruga, H. Tochiyama, and Y. Murata, Phys. Rev. Lett. **53**, 372 (1984).
- ⁶Y. Murata, H. Tochiyama, and M. Kubota, in Ref. 4; H. Tochiyama, M. Kubota, M. Miyao, and Y. Murata, Surf. Sci. **158**, 497 (1985); H. Tochiyama and Y. Murata, *ibid.* **215**, L323 (1989).
- ⁷E. M. Oellig and R. Miranda, Surf. Sci. **177**, L947 (1986); E. G. Michel, M. C. Asensio, and R. Miranda, in Ref. 1.
- ⁸E. M. Oellig, E. G. Michel, M. C. Asensio, R. Miranda, J. C. Duran, A. Munoz, and F. Flores, Europhys. Lett. **5**, 727 (1988); J. E. Ortega, E. M. Oellig, J. Ferron, and R. Miranda, Phys. Rev. B **36**, 6213 (1987).
- ⁹Y. Enta, T. Kinoshita, S. Suzuki, and S. Kono, Phys. Rev. B **36**, 9801 (1987); **39**, 1125 (1989).
- ¹⁰T. Abukawa and S. Kono, Phys. Rev. B **37**, 9097 (1988).
- ¹¹I. P. Batra, J. M. Nicholls, and B. Reihl, J. Vac. Sci. Technol. A **5**, 898 (1987).
- ¹²T. Kendelewicz, P. Soukiassian, R. S. List, J. C. Woicik, P. Pianetta, I. Lindau, and W. E. Spicer, Phys. Rev. B **37**, 7115 (1988); P. Soukiassian and T. Kendelewicz, in Ref. 4.
- ¹³G. S. Glander and M. B. Webb, Bull. Am. Phys. Soc. **33**, 570 (1988); Surf. Sci. **222**, 64 (1989); **224**, 60 (1990).
- ¹⁴Y. Enta, S. Suzuki, S. Kono, and T. Sakamoto, Phys. Rev. B **39**, 5524 (1989).
- ¹⁵P. Pervan, E. G. Michel, G. R. Castro, R. Miranda, and K. Wandelt, J. Vac. Sci. Technol. A **7**, 1885 (1989).
- ¹⁶E. G. Michel, R. Miranda, R. Ramirez, P. Pervan, G. R. Castro, and K. Wandelt (unpublished); also see Ref. 4.
- ¹⁷H. Tochiyama, Surf. Sci. (to be published).
- ¹⁸S. Ciraci and I. P. Batra, Phys. Rev. Lett. **56**, 877 (1986); Phys. Rev. B **37**, 2995 (1988); Ref. 4.
- ¹⁹M. Tsukada, H. Ishida, and N. Shima, Phys. Rev. Lett. **53**, 376 (1984); H. Ishida, N. Shima, and M. Tsukada, Phys. Rev. B **32**, 6236 (1985).
- ²⁰M. Tsukada, N. Shima, Z. Zhu, H. Ishida, and K. Terakura, in Ref. 4.
- ²¹R. V. Kasowski and M. H. Tsai, Phys. Rev. Lett. **60**, 546 (1988). See response to this Comment by S. Ciraci and I. P. Batra, Phys. Rev. Lett. **60**, 547 (1988).
- ²²P. S. Bagus and I. P. Batra Surf. Sci. **206**, L895 (1988); I. P. Batra and P. S. Bagus, J. Vac. Sci. Technol. A **6**, 600 (1988).
- ²³I. P. Batra, Phys. Rev. B **39**, 3919 (1989).
- ²⁴Y. Ling, A. J. Freeman, and B. Delley, Phys. Rev. B **39**, 10 144 (1989).
- ²⁵R. Ramirez, Phys. Rev. B **40**, 3962 (1989).
- ²⁶For some recent reviews, see I. P. Batra, Surf. Sci. **25**, 175 (1987); J. Chim. Phys. **86**, 689 (1989); *Physics and Chemistry of Alkali Metal Adsorption*, edited by H. P. Bonzel, A. M. Bradshaw, and G. Ertl (Elsevier, New York, 1989).
- ²⁷R. L. Gerlach and T. N. Rhodin, Surf. Sci. **19**, 403 (1970).
- ²⁸N. D. Lang, Phys. Rev. B **4**, 4234 (1971).
- ²⁹J. P. Muscat and I. P. Batra, Phys. Rev. B **34**, 2889 (1986); P. A. Serena, J. M. Soler, N. Garcia, and I. P. Batra, *ibid.* **36**, 3452 (1987).
- ³⁰E. Wimmer, A. J. Freeman, J. R. Hiskes, and A. M. Karo, Phys. Rev. B **28**, 3074 (1983); H. Ishida and K. Terakura, *ibid.* **38**, 5752 (1988).
- ³¹W. Mönch, J. Vac. Sci. Technol. B **4**, 1085 (1986).
- ³²T. M. Wong, D. Heskett, N. J. Dinardo, and E. W. Plummer, Surf. Sci. **208**, L1 (1989).
- ³³J. D. Levine, Surf. Sci. **34**, 90 (1973).
- ³⁴R. Holtom and P. M. Gundry, Surf. Sci. **63**, 263 (1977).
- ³⁵I. Langmuir, Phys. Rev. **23**, 112 (1924).
- ³⁶R. W. Gurney, Phys. Rev. **47**, 479 (1935).
- ³⁷B. Woratschek, W. Sesselman, J. Küppers, G. Ertl, and H. Haberland, Phys. Rev. Lett. **55**, 1231 (1985).
- ³⁸B. Goldstein, Surf. Sci. **35**, 227 (1973).
- ³⁹P. N. First, R. A. Dragoset, J. A. Strosio, R. J. Celotta, and R. M. Feenstra, J. Vac. Sci. Technol. A **7**, 2868 (1989).
- ⁴⁰T. Hashizume, Y. Hasegawa, I. Kamiya, T. Ide, I. Sumita, S. Hyodo, and T. Sakurai, J. Vac. Sci. Technol. A **8**, 233 (1990).
- ⁴¹P. Badt, A. Brodde, St. Tosch, and H. Neddermeyer, J. Vac. Sci. Technol. A **8**, 251 (1990).
- ⁴²F. Sette, T. Hashizume, F. Comin, A. A. McDowell, and P. H. Citrin, Phys. Rev. Lett. **61**, 1384 (1988).
- ⁴³M. T. Yin and M. L. Cohen, Phys. Rev. B **24**, 2303 (1981); D. J. Chadi, Phys. Rev. Lett. **43**, 43 (1979); K. C. Pandey, in *Proceedings of the 17th International Conference on the Physics of Semiconductors*, edited by D. J. Chadi and W. A. Harrison (Springer, Berlin 1984), p. 55.
- ⁴⁴F. F. Abraham and I. P. Batra, Surf. Sci. **163**, L752 (1985).
- ⁴⁵I. P. Batra, Phys. Rev. B **41**, 5048 (1990).
- ⁴⁶I. P. Batra, Phys. Rev. Lett. **63**, 1704 (1989).
- ⁴⁷J. Nogami, S. Park, and C. F. Quate, Appl. Phys. Lett. **53**, 2086 (1988); B. Bourguignon, K. L. Carleton, and S. R. Leone, Surf. Sci. **204**, 455 (1988).
- ⁴⁸D. H. Rich, A. Samsavar, T. Miller, H. F. Lin, T.-C. Chiang, J.-E. Sundgren, and J. E. Greene, Phys. Rev. Lett. **58**, 579 (1987).
- ⁴⁹J. Ihm, A. Zunger, and M. L. Cohen, J. Phys. C **12**, 4409 (1979).
- ⁵⁰K. C. Pandey, Phys. Rev. Lett. **49**, 223 (1982); M. Schlüter, J. R. Chelikowsky, S. G. Louie, and M. L. Cohen, Phys. Rev. B **12**, 4200 (1975).
- ⁵¹C. B. Bachelet, D. R. Hamann, and M. Schlüter, Phys. Rev. B **26**, 419 (1982).
- ⁵²D. M. Ceperley and B. J. Alder, Phys. Rev. Lett. **45**, 566 (1980).
- ⁵³J. P. Perdew and A. Zunger, Phys. Rev. B **23**, 5048 (1981).
- ⁵⁴I. P. Batra, S. Ciraci, G. P. Srivastava, J. S. Nelson, and C. Y. Fong, Phys. Rev. B **34**, 8246 (1986).
- ⁵⁵P. Bendt and A. Zunger, Phys. Rev. Lett. **50**, 1684 (1983).
- ⁵⁶P. Soukiassian, M. H. Bakshi, Z. Hurych, and T. M. Gentle, Surf. Sci. **221**, L759 (1989).
- ⁵⁷I. P. Batra, Phys. Rev. B **42**, 9162 (1990).
- ⁵⁸C. M. Wei, H. Huang, S. Y. Tong, G. S. Glander, and M. B. Webb, Phys. Rev. B **42**, 11 284 (1990).
- ⁵⁹H. Ishida and K. Terakura, Phys. Rev. B **40**, 11 519 (1989).
- ⁶⁰T. Abukawa, Y. Enta, T. Kashiwakura, S. Suzuki, S. Kono, and T. Sakamoto, J. Vac. Sci. Technol. A **8**, 3205 (1990).